Molecular Crystals and Liquid Crystals
Publication details, including instructions for authors and subscription information:
http://www.tandfonline.com/loi/gmcl20

Nuclear Magnetic Resonance Study of Hydrated Bentonite

J. P. Donoso [a], C. E. Tambelli [a], C. J. Magon [a], R. I. Mattos [a], I. D. A. Silva [a], J. E. de Souza [a], M. Moreno [a b], E. Benavente [b] & G. Gonzalez [c]

[a] Instituto de Física de São Carlos, Universidade de São Paulo, São Carlos, SP, Brasil

[b] Departamento de Química, Universidad Tecnológica Metropolitana, Santiago, Chile; Center for the Development of Nanoscience and Nanotechnology, CEDENNA

[c] Departamento de Química, Facultad de Ciencias, Universidad de Chile, Santiago, Chile; Center for the Development of Nanoscience and Nanotechnology, CEDENNA

Version of record first published: 28 May 2010

To cite this article: J. P. Donoso, C. E. Tambelli, C. J. Magon, R. I. Mattos, I. D. A. Silva, J. E. de Souza, M. Moreno, E. Benavente & G. Gonzalez (2010): Nuclear Magnetic Resonance Study of Hydrated Bentonite, Molecular Crystals and Liquid Crystals, 521:1, 93-103

To link to this article: http://dx.doi.org/10.1080/15421401003723219

Mol. Cryst. Liq. Cryst., Vol. 521: pp. 93–103, 2010

ISSN: 1542-1406 print/1563-5287 online
DOI: 10.1080/15421401003723219

Taylor & Francis
Taylor & Francis Group

Nuclear Magnetic Resonance Study of Hydrated Bentonite

J. P. DONOSO,[1] C. E. TAMBELLI,[1] C. J. MAGON,[1] R. I. MATTOS,[1] I. D. A. SILVA,[1] J. E. DE SOUZA,[1] M. MORENO,[1,2] E. BENAVENTE,[2] AND G. GONZALEZ[3]

[1]Instituto de Física de São Carlos, Universidade de São Paulo, São Carlos, SP, Brasil
[2]Departamento de Química, Universidad Tecnológica Metropolitana, Santiago, Chile; Center for the Development of Nanoscience and Nanotechnology, CEDENNA
[3]Departamento de Química, Facultad de Ciencias, Universidad de Chile, Santiago, Chile; Center for the Development of Nanoscience and Nanotechnology, CEDENNA

Impedance spectroscopy and nuclear magnetic resonance (NMR) were used to investigate the mobility of water molecules located in the interlayer space of H^+ – exchanged bentonite clay. The conductivity obtained by ac measurements was 1.25×10^{-4} S/cm at 298 K. Proton (^1H) lineshapes and spin-lattice relaxation times were measured as a function of temperature over the temperature range 130–320 K. The NMR experiments exhibit the qualitative features associated with the proton motion, namely the presence of a ^1H NMR line narrowing and a well-defined spin-lattice relaxation rate maximum. The temperature dependence of the proton spin-lattice relaxation rates was analyzed with the spectral density function appropriate for proton dynamics in a two-dimensional system. The self-diffusion coefficient estimated from our NMR data, $D \sim 2 \times 10^{-7}$ cm^2/s at 300 K, is consistent with those reported for exchanged montmorillonite clay hydrates studied by NMR and quasi-elastic neutron scattering (QNS).

Keywords Bentonite; clays; EPR; impedance spectroscopy; NMR; proton conduction; water adsorbed

Introduction

During the past decade natural clays have attracted considerable attention because of their large surface area and ion exchange properties. Layer-structured clay minerals have been characterized by their large adsorption capacity in the interlayer space. The water adsorption properties of natural lamellar clay minerals are induced by the presence, in the interlamellar space, of ions (exchangeable cations) balancing

Address correspondence to J. P. Donoso, Instituto de Física de São Carlos, Universidade de São Paulo, São Carlos, SP, Brasil. E-mail: donoso@ifsc.usp.br

structural and electrical deficiencies [1,2]. Bentonite is a laminar natural aluminosilicate that can occlude one or two molecular diameter-thick water films within an interlamellar space. Bentonites are rocks dominated by smectites group minerals, which include sodium and calcium montmorillonite, saponite, beidellite and hectorite. The smectite is a layered clay mineral constituted by two silica tetrahedral sheets bonded to a central alumina octahedral sheet. Basal spacing for air dried smectites changes from 1.26 to 1.54 nm depending on the type and valence of the exchangeable cation. Hydrated layered clays are considered proton conductors. The ionic conductivity arises from the diffusion of protons through the interlayer space giving rise to a room temperature conductivity of about 10^{-3} to 10^{-5} S/cm [2–4].

Clays are often used as additive in polymers for improving their mechanical and physicochemical properties [5]. During the last years, clay/polymer composites useful for ion-conducting membranes in batteries [6] and fuel cells have deserved much attention. It has been reported, for instance, that ionic conductivity in poly (ethylene oxide) based polymer electrolytes increases several orders of magnitude by the addition of 1–20% of bentonite [7]. Montmorillonite particles also result useful in regulating methanol crossover and proton conductivity of Nafion® [8,9] or crosslinked poly(vinyl alcohol) (PVA) [10] membranes for fuel cells. Their results are generally promising; however, in spite that the presence of clay increases significantly the barrier to methanol migration, the proton conductivity is reduced. Such results could surely be further improved by modifying the interlamellar spaces of the additive, especially by enhancing proton conductivity in the clay.

Nuclear magnetic resonance (NMR) is a well-known element-selective experimental technique used to study proton dynamics [3]. Being capable to probe magnetic and electric local interactions, measurements of NMR line shapes and spin-attice relaxation times as a function of temperature, provide important information on the proton mobility. In the last two decades, NMR techniques have been extensively used to study the coordination and the mobility of the water intercalated in lamellar clay minerals.

In recent years, a number of magnetic resonance studies have addressed the structural role of water adsorbed on clays. Reported NMR studies were reviewed by Sposito [11] and Whittingham [12]. Early investigations used the NMR technique to determine the structural role of water and the protonic motion in hydrate exchangeable clays. Hougardy *et al.* reported a ^{1}H and ^{2}H NMR study of adsorbed water in the layered silicate Na-vermiculite. The NMR linewidth and spin-lattice relaxation temperature dependence were attributed to rotational diffusion motion of the hydration shell and – above 270 K – to the diffusion of water in the interlamellar spaces. The proton lineshape and spin relaxation was found to be affected by the presence of Fe^{3+} paramagnetic centers [13]. Slade *et al.* investigated the protonic conduction in Na^+, Li^+ and Ni^{2+} exchanged montmorillonite clays with 13 wt% water content by conductivity as well as by ^{1}H NMR spin-lattice (T_1) and spin-spin (T_2) relaxation time measurements. The dominant relaxation mechanism was attributed to the modulation of the dipolar interaction between the ^{1}H nuclear spin and the electronic spin of the paramagnetic Fe^{3+}. Using the two-dimensional random walk equation and the correlation time obtained from the NMR experiments $\tau \approx 3 \times 10^{-9}$ s at 293 K, the authors estimated a diffusion coefficient of the order of $\sim 10^{-7}$ cm^2/s at this temperature [4]. Ishimaru *et al.* examined the dynamics of intercalated water in D_2O saturated synthetic saponite and in synthetic and natural smectites and Na-fluormica by measurements of ^{2}H and ^{7}Li NMR spectra and relaxation times. The results in

D_2O saturated Li-saponite indicate that the ^2H relaxation was governed by a single molecular motion described by an Arrhenius correlation time with an activation energy $\underline{E} = \underline{0.43\,eV}$ (41.5 KJ/mol). The NMR spin lattice relaxation curves in the smectites were explained by assuming the existence of two motional modes, a C_2 rotation and an isotropic rotation of the D_2O molecules [14,15]. The same interpretation was asserted by Sanz *et al.*, who investigated the arrangement and mobility of water in vermiculite hydrates by means of ^1H NMR relaxation time measurements between 150 K and 370 K [16]. Nagashima examined the influence of magnetic impurities on the proton spectra and spin relaxation of water in kaolin clay [17] and Labouriau *et al.* described the spin-lattice relaxation of ^{29}Si in natural clays by considering the coupling of nuclear spins to fixed paramagnetic impurities in the absence of spin diffusion [18]. Recently, Tenorio *et al.*, examined the geometry of water molecules in Na-fluorhectorite clay hydrates by ^1H and ^2H NMR spectroscopy [19].

The NMR techniques were also used to investigate water diffusivity in clay suspensions and in saturated compacted clays. The study of water diffusivity in water-rich bentonite is essential to the design of engineered barriers for underground disposal of nuclear waste [20,21]. Porion *et al.* reported water self-diffusion measurements of dense aqueous suspensions of synthetic laponite clays by ^1H pulse field gradient NMR technique [22] and Fagan *et al.* used an NMR bio-medical imaging system to study the diffusion of water in bentonite [23]. Ohkubo *et al.* reported a ^1H NMR investigation of water in saturated compacted bentonites [20] and Guichet *et al.* used the pulse field gradient NMR technique to determine water diffusivity in Na-smectite clay suspensions [21]. All these results mainly concern clays with alkaline or alkaline earth cations, but reports on clays in its proton form are still scarce.

In this work, the dynamics of intercalated water in the ion-exchanged H^+-bentonite is investigated by impedance spectroscopy and nuclear magnetic resonance (NMR). Continuous wave electron paramagnetic resonance (CW-EPR) was used to identify paramagnetic impurities in the bentonite samples. The EPR spectra indicate the presence of a strong signal at $g = 4.2$ which was ascribed to Fe^{3+} located in the interior of the clay sheets. Results indicate that the ^1H NMR behavior is strongly modified by the presence of water.

Experimental

Purification and Characterization NA-Bentonite. Pristine bentonite obtained from Sigma was first purified by sedimentation techniques and then converted to the sodium form by ionic exchange with 1 M sodium chloride. The salt excess was separated by dialysis (Sigma dialysis tubing cellulose membrane). The mean particle size of the product after filtering the suspension with a membrane (Whatman glass micro fiber filters, GF/D) was less than 3 μm. The stoichiometry of the obtained Na-bentonite, $Na_{0.47}(Al_{1.58}Fe_{0.17}Mg_{0.25})(Al_{0.22}Si_{3.78}O_{10})(OH)_2 \cdot nH_2O$, was determined by Plasma Atomic Absorption Spectroscopy (Perkin Elmer ICP-OES OPTIMA 1000DV). The sodium content corresponds to a cation exchange capacity (*cec*) of 85 meq per 100 g of the clay. The *cec* of Na-bentonite was corroborated by determining the exchange of sodium with an ethylenediamine complex of Cu(II) [24].

Preparation of the H-Bentonite. 2-g of Na-Bentonite was treated with HCl 0,1 M solutions three times, lasting 5 h each, under stirring at room temperature. After

each treatment, the clay suspension was centrifuged and the final product washed with distilled water and dried under vacuum for 12 h at room temperature. The titration with NaOH (phenolphthalein) points to an exchange capacity of 80 meq H^+/g dried clay. This value is very close to sodium content in the parent Na^+-form thus showing that the exchange process occurrs without significant alteration of the elemental composition of the aluminosilicate lattice. X-ray analyses carried out before and after protonation process did not show any significant change indicate that the crystallographic structure is also preserved (Fig. 1).

In each NMR experiment, the sample powder was dried in air at 60°C for 48 h and was then exposed to saturated water vapor for 24 h at 40°C. This time span was found to be sufficient to reach a stable hydration state. The amount of water absorbed was determined by weighing the sample in an analytical balance. For the sample of H^+-bentonite studied here, 5.39 water molecules were absorbed per unit cell (28% relative to the dry material mass). The hydrated sample was characterized by thermogravimetric analysis (TGA) (Shimadzu, model TGA-50, heating rate 10^o/min.) between room temperature and 800 K (Fig. 2). The curve of weight loss vs. temperature indicates that the slightly linked adsorbed water is removed in the first stage 25–120°C. The weight loss of 2.5% in the range of 120–350°C, which in cation exchanged bentonites is assigned to the elimination of the water coordinated to the interlayer cations [25,26], should correspond in our case to the hydration water at the proton. Finally, the weight loss of 4.7% in the range of 350–700°C should originate from the structural dehydration of neighboring hydroxyl groups.

Conductivity measurements were performed on powder samples pressed into cylindrical pellets (6 mm diameter and 1.5 mm thickness) at 60 kgf/cm^2. The sample was mounted in a sealed cell maintained at 298 K. Complex impedance measurements were conducted in the $1\,\text{Hz} - 1\,\text{MHz}$ frequency range, using a *Solartron* impedance analyzer (model 1260). The measured conductivity at 298 K in the hydrated sample was $\sigma = 1.25 \times 10^{-4}\,\text{S/cm}$.

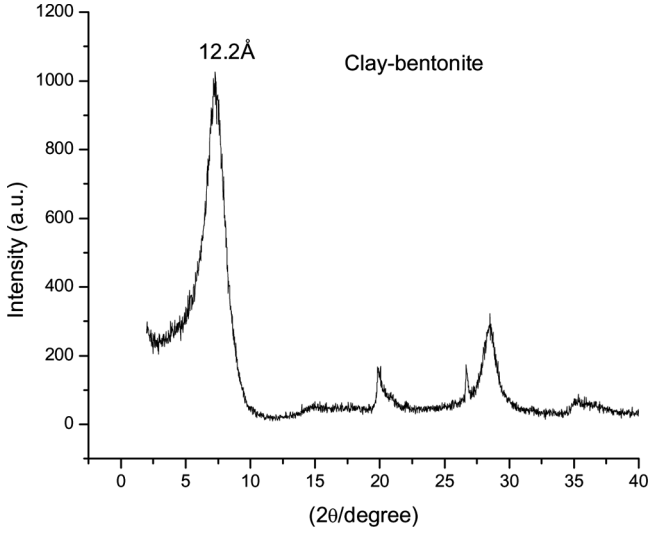

Figure 1. X-Ray difraction patterns of H^+-bentonite.

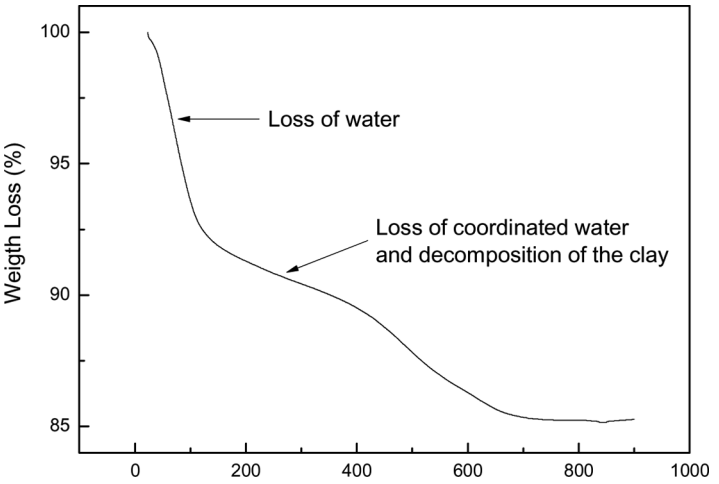

Figure 2. Thermogravimetric analysis (TGA) of the H^+ form of hydrated bentonite between room temperature and 800 K.

Electron paramagnetic resonance experiments were carried out at X-band frequency (≈9.5 GHz), using a Bruker E580 spectrometer. Proton ^1H NMR linewidth and spin-lattice relaxation measurements were carried out in the powder samples from 130 K to 320 K using a home-built pulsed NMR spectrometer operating at 36 MHz, equipped with a TECMAG NMR-kit, where a typical non-selective $\pi/2$ pulse length was of about 2 μs. Spin-lattice relaxation times were determined using the standard saturation-recovery method. The ^1H lineshape was obtained from the Fourier transform of the free induction decay generated by a $\pi/2$ pulse after 16 accumulations.

Results and Discussion

Proton NMR lineshapes and spin-lattice relaxation times of the hydrated bentonite were measured in the temperature range between 130 K and 320 K. The low temperature ^1H NMR spectrum of clay hydrates and layered protonic conductor consists typically of a narrow central line flanked by a pair of peaks (Pake doublet) arising from the intramolecular dipolar interactions between H-H spin pairs belonging to protonic species, such as H_2O molecules, OH^- and H_3O^+ ions [13,16,19,27,28]. However, the ^1H spectra of our hydrated H^+-bentonite clay measured at temperatures lower than 180 K show a lineshape consisting of a relatively narrow central line ($\Delta\upsilon \leq 5$ kHz) superimposed on a broad base line ($\Delta\upsilon \approx 80$ kHz). The fact that a Pake doublet is not observed suggests that a proton exchange mechanism is operating within the water molecules of the hydration shell [13,29]. A similar ^1H spectrum is observed for a dry H^+-bentonite sample, with the linewidth of the broad line on the order of $\Delta\upsilon \approx$ 55 kHz. This broad line observed at temperatures lower than 150 K in the dry sample is attributed to rigid protons and bound water in the structure. Figure 3 shows the temperature dependence of the broad linewidth of the ^1H NMR spectrum. As seen in Figure 3, above 180 K the proton mobility averages out the proton–proton dipolar interactions and the ^1H NMR line narrows. Intra- and inter-molecular dipolar interactions between protons are reduced by local molecular motions, such as H_2O

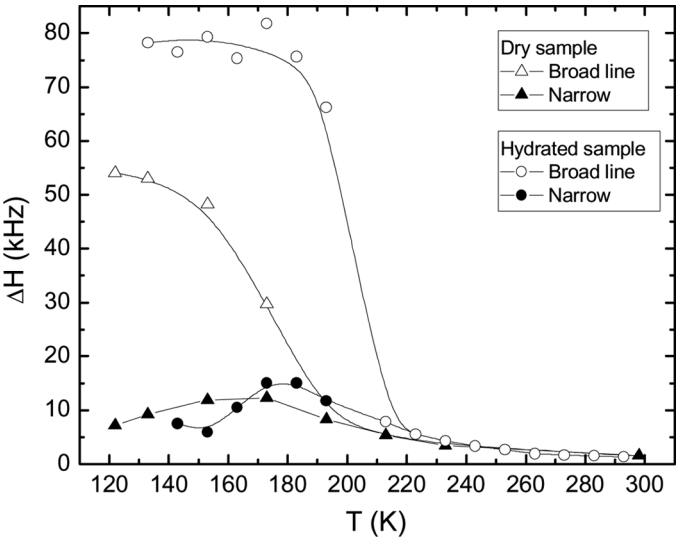

Figure 3. Temperature dependence of the ^{1}H NMR linewidth of the H^+ form of dry and hydrated bentonite. Solid lines are guides to the eyes.

rotations and proton diffusion. The motional narrowing of the NMR line takes place when the rate of the fluctuations of the local dipolar fields, which is generally described by a correlation time τ, is on the order of the rigid lattice linewidth. Assuming a thermally activated process following an Arrhenius law, $\tau = \tau_o \exp(E_a/kT)$, where E_a is the activation energy (i.e., the barrier height), k is the Boltzmann constant and τ_o^{-1} is a pre-exponential factor, the activation energy of the line narrowing process can be estimated from the onset temperature (T_c) using the semi-empirical Waugh-Fedim expression [30]:

$$E_a(eV) = 1.617 \times 10^{-3} T_c(K) \tag{1}$$

The Waugh-Fedin method is useful when the onset temperature of the motional narrowing process can be located and the full range of the line narrowing cannot be determined. The analysis of the line narrowing data in Figure 3 with Eq. (1) yields a activation energy of 0.3 eV (29 KJ/mol).

Figure 4 shows the temperature dependence of the proton spin-lattice relaxation rates (T_1^{-1}). The relaxation recovery was found to be exponential throughout the temperature range. The relaxation curve shows a symmetrical V-shape curve, with a relaxation rate maximum at around 235 K. The spin-lattice relaxation rate can be expressed in terms of the spectral density function evaluated at the NMR Larmor frequencies ω_o of the nuclei with spin I [31]:

$$\frac{1}{T_1} = C[J(\omega_o\tau) + 4J(2\omega_o\tau)] \tag{2}$$

where $J(\omega)$ is the spectral density function, which is parameterized by the Larmor frequency, ω_o, and the correlation time, τ, of the proton motion modulating the spin interactions. The constant C in Eq. (2) depends on the spin interaction responsible for the relaxation. The measured value of the ^{1}H relaxation time in the hydrated

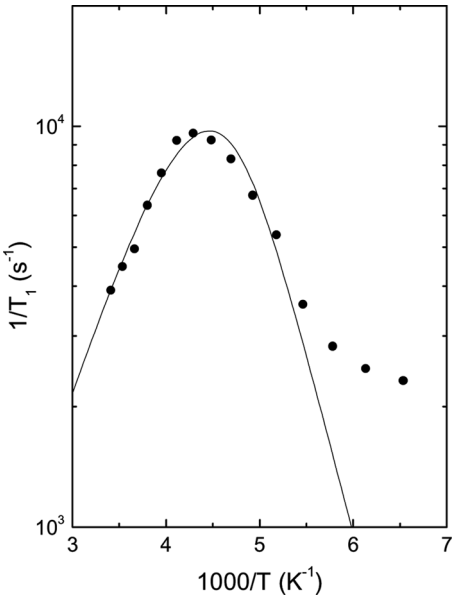

Figure 4. Temperature dependence of the ^{1}H spin-lattice relaxation rates (solid dots) of the H^+ form of hydrated bentonite measured at the Larmor frequency of 36 MHz. Solid line is calculated using a 2D spectral density function Eq. (4).

H^+-bentonite (T_1 between 100 μs and 500 μs) is about three orders of magnitude smaller than the ^{1}H T_1 usually observed for H_2O in proton conductors in the same temperature region (T_1 between 30 ms and 500 ms) [4,26,32]. The modulation of the dipole-dipole couplings between the proton spins in the water molecules (^{1}H-^{1}H in H_2O) do not account for the measured relaxation rates in the hydrated H^+-bentonite. In the case of natural clays, the abnormally short spin-lattice relaxation times observed have been explained by considering the dipolar coupling of the ^{1}H nuclear spin with the electronic spin of paramagnetic impurities [4,13,33]. Figure 5 shows the room temperature EPR spectra of a pure Na^+-bentonite. Two prominent features, with effective g-values of ~4.2 and 2.0, appeared in the spectra. The former is attributed to isolated Fe^{3+} ions in tetrahedral or octahedral coordination and correspond to the iron located in the clay structure (iron substituting aluminum in octahedral layers) [34]. The relatively sharp resonance signal at $g \approx 2$ can be attributed to an oxygen paramagnetic center.

Therefore, the dominant relaxation mechanism of the ^{1}H NMR relaxation in the hydrate H^+-bentonite is the modulation of the dipolar interaction between the nuclear spin (^{1}H) and the electronic spin of the paramagnetic Fe^{3+}. According to the model of Resing and Thompson [35], the constant C of the spin interaction responsible for the proton relaxation, which measures the interaction strength between an ion and a nucleus is defined by [13,33,35],

$$C = \frac{4}{15}\gamma_e^2\hbar^2 S(S+1)\left(\frac{4\pi N}{\lambda^3}\right) \tag{3}$$

where λ is the mean distance between the proton and the Fe^{3+}, $\gamma_e = 3.8 \times 10^7\ (\mathrm{G\,s})^{-1}$ is the gyromagnetic ratio of the electronic spins for $g = 4.2$, and N is the

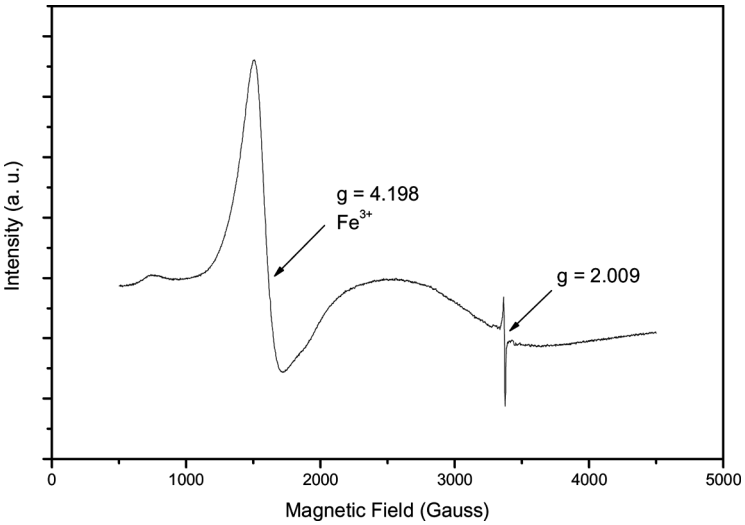

Figure 5. Electron paramagnetic resonance (EPR) spectrum of a pure bentonite sample. The spectrum was obtained at room temperature. The EPR analysis indicates the presence of isolated Fe^{3+} in tetrahedral or octahedral coordination (signal at $g = 4.3$).

concentration of paramagnetic centers. Using the measured spin-relaxation maximum in Figure 4, $T_1^{-1} \approx 10^4\,s^{-1}$ at 235 K, and assuming that Fe^{3+} can be present in the Al sites of the clay structure, we estimate the Fe^{3+} concentration as $N \approx 5 \times 10^{19}\,cm^{-3}$. This value has the same order of magnitude of the impurity concentration determined by chemical analysis in hectorite and montmorillonite natural clays [18].

In the case of dynamical processes in a reduced dimensionality, which is relevant in the case of the diffusive motion of water molecules within layered structures, the spectral density function $J(\omega_o,\tau)$ for diffusion in two dimensions is given by the expression [27,29]:

$$J(\omega_o\tau) \propto \ln\left(1 + \frac{1}{\omega_o^2\tau^2}\right) \tag{4}$$

The solid line in Figure 4 shows the fitting of the data by the spectral density, Eq. (4), using $E_A = 0.18$ eV, and $\tau_o \approx 1 \times 10^{-12}$ s. The position of the relaxation rate maximum $(T_1^{-1})_{max}$, predicted by Eqs. (2) and (4), indicates the temperature, T_{max}, at which the motional correlation time is comparable to the reciprocal of the ^1H Larmor frequency. For the hydrate H^+-bentonite, $T_{max} = 235$ K and $\tau(235) \approx 4 \times 10^{-9}$ s. Only one relaxation rate maximum is observed in the temperature window analyzed. However, Sanz *et al.* reported the presence of two possible relaxation mechanisms in Na-vermiculite hydrates. The relaxation time minimum $(T_1)_{min}$ observed at a higher temperature (i.e., $T \approx 313$ K) was assigned to hopping/diffusion of water molecules between equivalent sites and the second one observed at a lower temperature (i.e., $T \approx 233$ K) was attributed to the residual rotation of water molecules around the C_2 axis [16].

The motional parameters obtained from the relaxation data allow us to estimate the proton self-diffusion coefficient by means of the well-known random walk expression:

$$D = \frac{l^2}{2\alpha\tau} \tag{5}$$

Here $\alpha = 1$, 2 or 3, depending on the dimensionality of the motion and l, is the mean-square displacement as calculated from the intersite jump length ($l \approx 3$ Å) [4,29]. By taking $\tau(300\,\mathrm{K}) \approx 10^{-9}$ s, $l = 3$ Å and $\alpha = 2$ for two-dimensional diffusion process, we obtained $D \sim 2 \times 10^{-7}\,\mathrm{cm}^2/\mathrm{s}$. This value is consistent with those reported for Ni^{2+}-exchanged montmorillonite hydrate with about 13% water content, $D(293\,\mathrm{K}) \sim 10^{-7}\,\mathrm{cm}^2/\mathrm{s}$ [4] and for hydrated layered chalcogenides, $A^{+}(H_2O)_y\{MX_2\}$; A = Li, Na, K, Rb and M = Nb, S and Ta, $D \sim 1.6 \times 10^{-7}\,\mathrm{cm}^2/\mathrm{s}$ [29]. Moreover, our result is also consistent with the diffusion coefficient at room temperature measured by quasi-elastic neutron scattering (QNS) for Ca^{2+}-exchanged motmorillonite, $D \sim 1.1 \times 10^{-7}\,\mathrm{cm}^2/\mathrm{s}$ [36] and for Li-exchanged smectites, $D \sim 6.6 \times 10^{-7}\,\mathrm{cm}^2/\mathrm{s}$ [37]. Taking into account that the conductivity of exchanged montmorillonite hydrate clays is strongly dependent on water content [2], the agreement observed between these diffusion coefficient values is highly satisfactory.

Conclusions

The ^{1}H NMR spectra and dynamics of proton are strongly influenced by the presence of Fe^{+3} ions resulting from isomorphic exchange of Si^{+4} in the bentonite octahedral layers. Thus, the dominant relaxation mechanism of the ^{1}H NMR relaxation in the clay is the modulation of the dipolar interaction between the nuclear spin (^{1}H) and the electronic spin of the paramagnetic ion Fe^{3+}. The influence of the hydration degree on the ^{1}H NMR behavior of H^+-bentonite is similar to that observed in cationic-bentonites. In both cases, the presence of an excess of water is necessary for obtaining relatively high proton diffusion coefficients. The increase in the interlaminar distance accompanying water excess, about 2 Å, is not enough for the formation of a second hydration layer, so that excess of water is expected to occupy the space generated between the hydrated cationic centers that are neutralizing the intrinsic negative charges upon the clay lamellae. According to the *cec* of our bentonite (about 0.47 equivalent per Si_4 unit) and assuming a statistic distribution, ionic centers in clay interlaminar space are each other relatively far, about 10 Å. Therefore, enhanced conductivity promoted by water excess is probably due to water-bridges between the hydration shells of positive ions in the interlaminar space. Interestingly, in the case of the proton the exchange between different water species is more extended, thus being those species indistinguishable in the time scale of the NMR experiments. This fact is in contrast with metal cation derivatives, in which the two different relaxation processes are assigned to hydration cation shell and free water, respectively. Such an exchange peculiarity, observed for hydrated bentonite in the H^+ form, makes this bentonite an interesting candidate for being used as inorganic additive in polymer electrolytes for batteries and fuel cell applications. However, to counteract the effect of charge localization on the clay sheets new architectures of the interlamellar space must be designed.

Acknowledgments

Partial support of CNPq and Fapesp (Brasil) are gratefully acknowledged. The authors are grateful to Dr. J. F. Lima for the EPR analysis. Research partially financed by FONDECYT (Contracts 1090282, 1070195), Basal Financing Program CONICYT, FB0807 (CEDENNA), Millenium Science Nucleus P06-022-F.

References

[1] Poinsignon, C. (1997). *Solid State Ionics*, *97*, 399.
[2] Aliouane, N., Hammouche, A., De Doncker, R. W., Telli, L., Boutahala, M., & Brahimi, B. (2002). *Solid State Ionics*, *148*, 103.
[3] Colomban, P. (1992). (Editor), *Proton Conductors*, Cambridge University Press: Cambridge, UK.
[4] Slade, R. C. T., Barker, J., Hirst, P. R., Halstead, T. K., & Reid, P. I. (1987). *Solid State Ionics*, *24*, 289.
[5] Pavlidou, S. & Papaspyrides, C. D. (2008). *Progress in Polymer Science*, *33*, 1119.
[6] Moreno, M., Santa Ana, M., González, G., & Benavente, E. *Electrochimica Acta*, *55*, 1323.
[7] Kim, S. & Park, S. J. (2007). *Solid State Ionics*, *178*, 973.
[8] Thomassin, J.-M., Pagnoulle, C., Caldarella, G., & Germain, R. Jerome. (2006). *Journal of Membrane Science*, *270*, 50.
[9] Hasani-Sadrabadi, M. M., Dashtimoghadam, E., Majedi, F. S., & Kabiri, K. (2009). *Journal of Power Sources*, *190*, 318.
[10] Kim, D. S., Park, I. C., Cho, H. Il., Kim, D. H., Moon, G. Y., Lee, H. K., & Rhim, J. W. (2009). *Journal of Industrial and Engineering Chemistry*, *15*, 265.
[11] Sposito, G. & Prost, R. (1982). *Chemical Reviews*, *82*(6), 553.
[12] Whittingham, M. S. (2004). *Solid State Ionics*, *168*, 255.
[13] Hougardy, J., Stone, W. E. E., & Fripiat, J. J. (1976). *J. Chemical Physics*, *64*, 3840.
[14] Ishimaru, S. & Ikeda, R. (1997). *Z. Naturforsch*, *52a*, 863.
[15] Ishimaru, S. & Ikeda, R. (1999). *Z. Naturforsch*, *54a*, 431.
[16] Sanz, J., Herrero, C. P., & Serratosa, J. M. (2006). *J. Physical Chemistry B*, *110*, 7813.
[17] Nagashima, K. (2006). *Applied Magnetic Resonance*, *30*, 55.
[18] Laboriau, A., Kim, Y.-W., & Earl, W. L. (1996). *Physical Review B*, *54*, 9952.
[19] Tenorio, R., Alme, L. R., Engelsberg, M., Fossum, J. O., & Hallwas, F. (2008). *J. Physical Chemistry C*, *112*, 575.
[20] Ohkubo, T., Kikuchi, H., & Yamaguchi, M. (2008). *Physics and Chemistry of the Earth*, *33*, S169.
[21] Guichet, X., Fleury, M., & Kohler, E. (2008). *J. Colloid & Interface Science*, *327*, 84.
[22] Porion, P., Al Mukhtar, M., Faugere, A. M., Pellenq, R. J. M., Meyer, S., & Delville, A. (2003). *J. Phys. Chem. B*, *107*, 4012.
[23] Fagan, A. J., Nestle, N., & Lurie, D. J. (2005). *Magnetic Resonance Imaging*, *23*, 317.
[24] Bergaya, F. & Vayer, M. (1997). *Applied Clay Science*, *12*, 275.
[25] Caglar, B., Afsin, B., Tabak, A., & Eren, E. (2009). *Chemical Engineering Journal*, *149*, 242.
[26] Hassan, M. S. & Abdel-Khalek, N. A. (1998). *Appl. Clay Sci.*, *13*, 99.
[27] Mangamma, G., Bhat, V., Gopalakrishnan, J., & Bhat, S. V. (1992). *Solid State Ionics*, *58*, 303.
[28] Arribart, H. & Piffard, Y. (1983). *Solid State Communications*, *45*, 571.
[29] Röder, U., Müller-Warmuth, W., Spiess, H. W., & Schöllhorn, R. (1982). *J. Chem. Phys.*, *77*, 4627.
[30] Wilkening, M., Bork, D., Indris, S., & Heitjans, P. (2002). *Phys. Chem. Chem. Phys.*, *4*, 3246.

[31] Abragam, A. (1961). *Principles of Nuclear Magnetism*, Oxford University Press: London, UK.
[32] Röder, U., Müller-Warmuth, W., & Schöllhorn, R. (1979). *J. Chem. Phys.*, *70*, 2864.
[33] Slade, R. C. T., Fridd, P. F., Halstead, T. K., & McGeehin, P. (1980). *J. Solid State Chem.*, *32*, 87.
[34] Carriazo, J. G., Molina, R., & Moreno, S. (2008). *Applied Catalysis A*, *334*, 168.
[35] Resing, H. & Thompson, J. K. (1967). *J. Chem Phys.*, *46*, 2876.
[36] Tuck, J. J., Hall, P. L., Hayes, M. H. B., Ross, D. K., & Poinsignon, C. (1984). *J. Chem. Society: Faraday Trans.*, *80*, 309.
[37] Poisignon, C., Estrade-Szwarckopf, H., Conard, J., & Dianoux, A. J. (1989). *Physica B*, *156/7*, 140.